Cite as: H. Zhang *et al.*, *Science* 10.1126/science.aaf2693 (2016).

NAD$^+$ repletion improves mitochondrial and stem cell function and enhances life span in mice

Hongbo Zhang,[1] Dongryeol Ryu,[1] Yibo Wu,[2] Karim Gariani,[1] Xu Wang,[1] Peiling Luan,[1] Davide D'Amico,[1] Eduardo R. Ropelle,[1,3] Matthias P. Lutolf,[4] Ruedi Aebersold,[2,5] Kristina Schoonjans,[6] Keir J. Menzies,[1,7]* Johan Auwerx[1]*

[1]Laboratory of Integrative and Systems Physiology, École Polytechnique Fédérale de Lausanne, 1015 Lausanne, Switzerland. [2]Department of Biology, Institute of Molecular Systems Biology, Eidgenössische Technische Hochschule Zürich (ETHZ), Zurich 8093, Switzerland. [3]Laboratory of Molecular Biology of Exercise, School of Applied Science, University of Campinas, CEP 13484-350 Limeira, São Paulo, Brazil. [4]Laboratory of Stem Cell Bioengineering, École Polytechnique Fédérale de Lausanne, 1015 Lausanne, Switzerland. [5]Faculty of Science, University of Zurich, Zurich, Switzerland. [6]Metabolic Signaling, École Polytechnique Fédérale de Lausanne, 1015 Lausanne, Switzerland. [7]Interdisciplinary School of Health Sciences, University of Ottawa Brain and Mind Research Institute, 451 Smyth Rd, K1H 8M5, Ottawa, Canada.

*Corresponding author. Email: kmenzies@uottawa.ca (K.J.M.); admin.auwerx@epfl.ch (J.A.)

Adult stem cells (SCs) are essential for tissue maintenance and regeneration yet are susceptible to senescence during aging. We demonstrate the importance of the amount of the oxidized form of cellular nicotinamide adenine dinucleotide (NAD$^+$) and its impact on mitochondrial activity as a pivotal switch to modulate muscle SC (MuSC) senescence. Treatment with the NAD$^+$ precursor nicotinamide riboside (NR) induced the mitochondrial unfolded protein response (UPR^{mt}) and synthesis of prohibitin proteins, and this rejuvenated MuSCs in aged mice. NR also prevented MuSC senescence in the *Mdx* mouse model of muscular dystrophy. We furthermore demonstrate that NR delays senescence of neural SCs (NSCs) and melanocyte SCs (McSCs), and increased mouse lifespan. Strategies that conserve cellular NAD$^+$ may reprogram dysfunctional SCs and improve lifespan in mammals.

In adults, tissue homeostasis is highly dependent on stem cell (SC) function. These adult SCs are not only essential in continuously-proliferating tissues, like the hematopoietic, intestinal and skin systems, but also in normally quiescent tissues, such as skeletal muscle and brain that require regeneration after damage or exposure to disease (*1*). Aging is accompanied by a decline in adult SC function, termed SC senescence, which leads to loss of tissue homeostasis and regenerative capacity (*2*, *3*).

Homeostasis and regeneration of skeletal muscle depends on normally quiescent muscle stem cells (MuSCs), which are activated upon muscle damage to expand and give rise to differentiated myogenic cells that regenerate damaged muscle fibers (*4*, *5*). These responses are blunted in aged muscle, probably because of reduced number and function of MuSCs (*6–8*). In aging, MuSC dysfunction may be caused by extrinsic signals (*9*, *10*) or intrinsic cellular senescence signaling pathways (*11*) or both. One general regulator of cellular senescence, cyclin-dependent kinase inhibitor 2A (CDKN2A, p16^{INK4A}), shows increased expression in geriatric MuSCs, which causes permanent cell cycle withdrawal and senescence of MuSCs in very old mice (28-32 months of age) (*11*). However, reductions in MuSC number and function can already be observed before this stage (*6*, *11*), indicating that MuSC senescence may be initiated at an earlier time point. Pre-geriatric mice, approximately two years old, can exhibit features of MuSC senescence (*8*, *12–15*). However, the early mechanisms that instigate MuSC senescence are still largely unknown.

One of the hallmarks of organismal aging is the appearance of mitochondrial dysfunction (*2*, *3*). Mitochondrial dysfunction, induced by calorie-dense diets or aging, can result from depletion of NAD$^+$ (the oxidized form of nicotinamide adenine dinucleotide), whereas NAD$^+$ repletion, with precursors such as nicotinamide riboside (NR), can reverse this process (*16–20*). Stem cells are thought to rely predominantly on glycolysis for energy, a process that would reduce cellular concentrations of NAD$^+$ (*21*). Mitochondrial function is linked to SC maintenance and activation (*22–25*), yet its role in senescence is unknown.

Mitochondrial dysfunction is a biomarker of MuSC senescence

To identify the role of mitochondrial function in SCs we compared MuSCs from young and aged mice to investigate SC senescence. To identify the principal mechanisms initiating MuSC senescence, we examined publically available MuSC gene expression datasets from young (~3 months) and aged (~24 months) mice using gene set enrichment analysis [GSEA; GEO dataset IDs: GSE47177 (*14*), GSE47104 (*12*) and GSE47401 (*8*)]. Enrichment scores of young *versus* aged datasets revealed upregulation of senescence pathways and downregulation of cell cycle pathways with age (Fig. 1A, tables S1 to S3, and fig. S1, A and B). This is consistent with

the idea that irreversible cell cycle arrest is a primary marker of cellular senescence (*2*, *3*). In all three datasets, tricarboxylic acid (TCA) cycle and oxidative phosphorylation (OXPHOS) pathways were among the most downregulated pathways in aged MuSCs (Fig. 1A, tables S1 to S3, and fig. S1, A and B). Analysis of gene ontology (GO) terms that were significantly (Gene Set Enrichment Analysis; FWER $p < 0.05$) downregulated in aged MuSCs, further demonstrated links to mitochondrial function (fig. S1C). Common downregulated genes during aging showed a substantial overlap (113 genes; 11.59%) with mitochondrial genes (*26*) (Fig. 1B and table S4), in contrast to the minimal (11 genes; 1.92%) overlap amongst common upregulated genes (fig. S1D and table S4). Among the 113 downregulated mitochondrial genes in aged MuSCs, 41.6% were related to the TCA cycle and OXPHOS (fig. S1E), which is higher than their percent composition of the whole mitochondrial proteome (~14%) (*27*, *28*). This indicates a dominant decline in expression of mitochondrial respiratory genes in aged MuSCs. The reduction in mitochondrial OXPHOS and TCA cycle genes was consistent for all independent datasets (fig. S1, F and G). We isolated primary aged and young MuSCs and confirmed reduced abundance of OXPHOS and TCA cycle transcripts (Fig. 1C), and reduced oxidative respiration rates in both freshly isolated (Fig. 1D) and cultured MuSCs (fig. S1H). MuSC mitochondrial dysfunction in aged mice was further confirmed by the loss of mitochondrial membrane potential (Fig. 1E) and a reduction in cellular ATP concentrations (Fig. 1F). Several important markers and regulators of the UPR^{mt}, a stress response pathway that mediates adaptations in mitochondrial content and function, were downregulated in aged MuSCs (fig. S1F and Fig. 1G). Despite the absence of consistent changes in cyclin-dependent kinase inhibitor 2A (CDKN2A) (fig. S1I and table S4) or mitogen-activated protein kinase 14 (MAPK14; p38) pathways (table S4), previously reported to regulate MuSC senescence, expression of cell cycle genes was decreased and expression of genes encoding the senescent proinflammatory secretome was increased (fig. S1, I to K). The reduction in cell cycle signaling was accompanied by increased expression of genes in the cyclin-dependent kinase inhibitor 1 (CDKN1A; $p21^{CIP1}$)-mediated pathway (fig. S1K and table S4), suggesting that early senescence in MuSCs may involve CDKN1A.

NAD^+ repletion improves MuSC function in aged mice

Given the importance of NAD^+ concentrations in the control of mitochondrial function (*16*, *29*), we examined the potential of NAD^+ repletion to improve MuSC numbers and muscle function in aged mice. Amounts of NAD^+ in freshly isolated MuSCs were lower in those isolated from aged mice and 6 weeks of NR treatment increased NAD^+ concentration in MuSCs from young and old mice (Fig. 2A). Amounts of NADH were relatively stable (fig. S2A). Muscle from aged mice contained fewer MuSCs (Fig. 2, B and C, and fig. S2, B and C). However, NR treatment increased MuSC numbers in young and old mice (Fig. 2, B and C, and fig. S2, B and C). The increase in MuSC numbers was confirmed with paired box protein Pax-7 (PAX7) staining, a known MuSC marker (*4*) (Fig. 2D and fig. S2, D and E). The effect of NR in young or aged mice appeared not to result from changes in muscle or body mass, as these measures remained comparable among all groups over the short treatment period (fig. S2, F to I). NR treatment also enhances muscle function in aged animals through an independent mechanism acting directly on the muscle fibers (*16*), as was apparent from improvements in maximal running times and distances, along with limb grip strength in aged mice (Fig. 2, E to G). Young animals showed no such changes (fig. S2, J to L).

Impairments in muscle regeneration efficiency have been linked to the decline in MuSC function in aged mice (*6*). We therefore examined the benefits of NR on muscle regeneration with cardiotoxin (CTX)-induced muscle damage (*4*). NR treatment accelerated muscle regeneration in aged and young mice (Fig. 2H and fig. S2M). NR-induced improvements in regeneration were paralleled by increases in PAX7-stained MuSCs in aged mice (Fig. 2I and fig. S2N), but not in young mice (fig. S2, O and P). NAD^+ repletion also improved the stemness of the aged MuSCs, as demonstrated by a reduction in myoblast determination protein 1 (MYOD1)-stained PAX7 immunostained cells (Fig. 2J and fig. S2Q), as MYOD1 is a transcriptional factor that activates MuSC differentiation. 7 days after CTX-induced damage, NR-treated aged mice exhibited improvements in embryonic myosin heavy chain staining, a protein expressed in fetal and newly regenerating adult muscle fibers (*30*) (Fig. 2K). When MuSCs were transplanted from NR-treated or control aged mice into *Mdx* mice (fig. S2R) (a mouse model of Duchenne muscular dystrophy that gradually loses MuSC function in aging due to the strain of continual muscle regeneration). MuSCs isolated from NR-treated donors more effectively replenished the MuSC compartment and stimulated myogenesis of dystrophin-positive myofibers when transplanted into either young or aged *Mdx* recipients (fig. S2S and Fig. 2L, respectively). Thus, NR treatment can both improve muscle regeneration and MuSC transplantation efficiency.

The inappropriate accumulation of non-myogenic fibro-adipogenic progenitors (FAPs) and inflammatory cells have been reported to impair MuSC function and muscle regeneration, especially in aged muscle or with chronic damage, as found in *Mdx* mice (*31*). NR treatment largely attenuated increases in FAP numbers 7 days after CTX induced damage in aged mice, but had no effect on FAPs under basal conditions (fig. S2, T to V). This effect is consistent with benefits

to FAP clearance in later periods of muscle regeneration (*31*). NR also alleviated macrophage infiltration 7 days after CTX induced regeneration in aged mice (fig. S2, W and X).

NR prevents MuSCs senescence by improving mitochondrial function

To explain the improvements in MuSCs from aged animals after NAD^+ repletion, we examined effects on MuSC senescence. Freshly isolated MuSCs from NR-treated young and aged mice were immunostained for phosphorylation of histone 2A.X at Ser139 (γH2AX), a marker of DNA damage (*2*). γH2AX-stained nuclei were more abundant in MuSCs from aged animals, and staining was reduced with NR treatment (Fig. 3, A and B, young controls found in fig. S3, A and B). The reduction of the nuclear damage response in MuSCs was confirmed by a single-cell gel electrophoresis (comet) assay, a sensitive measure of DNA strand breaks as an indicator of senescence (Fig. 3C), as well as by staining for β-galactosidase, another classical senescence marker (*2*) (fig. S3C). A 6-hour NR treatment of late passage C2C12 myoblasts also reduced the expression of cell senescence and apoptosis markers (*32*) (Fig. 3D). MuSCs isolated from NR-treated aged mice showed enhanced potential to form myogenic colonies (Fig. 3E and fig. S3D). Thus, NR exerts a protective effect against intrinsic MuSC senescence.

NR treatment of MuSCs from aged mice reduced abundance of mRNAs encoding CDKN1A and related proinflammatory proteins and increased the expression of cell cycle genes (Fig. 3F). These effects were not seen in non-senescent MuSCs from young animals (fig. S3E). NR treatment of MuSCs from aged animals increased expression of genes whose products function in the TCA cycle and OXPHOS (Fig. 3G), an effect that was not evident in young animals (fig. S3F). To quantify protein expression level at different conditions, we applied a new mass spectrometry-based proteomics technique, the sequential windowed acquisition of all theoretical fragment ion mass spectra (SWATH-MS) (*33*), which allows accurate and reproducible protein quantification across sample cohorts. Using this technique, we have quantified the expression changes of more than 1100 proteins in MuSCs across the various conditions. The SWATH-MS results show that a significant amount of proteins that function in OXPHOS and in the UPR^{mt} were decreased in MuSCs from aged animals (Fig. 3H and table S6). The overall amount of these same proteins was increased after NR supplementation (two-way AVOVA test, $p < 0.05$, Fig. 3H and table S6). Protein immuno-blotting of freshly isolated MuSCs from aged animals confirmed increased expression of proteins related to cell cycle and senescence that could not be detected by SWATH-MS (Fig. 3I).

MuSCs from NR treated aged mice exhibited increases in oxidative respiration (Fig. 3, J and K). NR-treated MuSCs from aged animals also showed increased mitochondrial membrane potential (Fig. 3L and fig. S3G) and increased abundance of ATP (Fig. 3M). To test whether this protective effect of NR on MuSC senescence relies on mitochondrial function we created a tamoxifen-inducible sirtuin-1 (SIRT1) MuSC-specific knockout mouse ($SIRT1^{MuSC-/-}$), by crossing $SIRT1^{flox/flox}$ mice with the $Pax7^{creER}$ strain. SIRT1 is an NAD^+-dependent deacetylase that increases mitochondrial biogenesis (*16*). The beneficial effect of NR on muscle regeneration after CTX injection appeared attenuated in $SIRT1^{MuSC-/-}$ mice (Fig. 3N). Supporting this qualitative observation, SIRT1-knockout in MuSCs blocked the beneficial effects of NR on MuSC activation (Fig. 3, O to Q) and senescence (Fig. 3R and fig. S3H) 7 days after regeneration. These data indicate that NR inhibits MuSCs senescence by improving mitochondrial function in a SIRT1-dependent manner. This finding is consistent with a report linking FOXO3 activation, a SIRT1 target, to improved mitochondrial metabolism in hematopoietic stem cells (*34*).

Rejuvenating MuSCs by activating the UPR^{mt} and prohibitin pathways

We further explored how UPR^{mt} might regulate senescence by examining the role of prohibitins, a family of stress response proteins. Prohibitins sense mitochondrial stress and modulate senescence in fibroblasts in mammals (*35*), maintain replicative lifespan in yeast (*36*), and promote longevity in worms (*37*), animals that lack adult SCs. Expression of prohibitins, *Phb* and *Phb2*, was reduced in the bioinformatics analysis (fig. S1F), and in freshly isolated aged MuSCs (fig. S4A). NR increased the expression of prohibitin proteins in C2C12 myoblasts (Fig. 4A) and transcripts in MuSCs of young and aged mice (Fig. 4B and fig. S4B). NR treatment was also shown to increase the expression of prohibitins concurrent to markers of UPR^{mt} and cell cycle (fig. S4C). Moreover, the overexpression of prohibitins, in the absence of NR, likewise increased UPR^{mt} and cell cycle protein expression (Fig. 4C). Demonstrating the dependency of the NR effect on prohibitins, improvements in UPR^{mt} and cell cycle protein expression were not observed with NR treatment following the knockdown of prohibitins (Fig. 4D and fig. S4D). To confirm the regulation of prohibitins on cell cycle proteins and to explore the effect of prohibitins on MuSC function, *Phb* was depleted in vivo through an intramuscular injection of *shPhb* lentivirus (PHB and PHB2 are functional only as a heterozygous protein complex) (*38*). Impairment of muscle regeneration and a reduction in MuSC numbers was observed in sh*Phb* lentivirus injected mice, 7 days after CTX-induced muscle regeneration (Fig. 4, E and F). Quantifying these results, *Phb* knockdown is shown to block the NR induced increase of MuSCs number upon regeneration (Fig. 4, G and H). Importantly, *Phb*

knockdown does not induce more MuSCs senescence in aged mice, yet prevents the beneficial effect of NR on MuSCs senescence (Fig. 4I and fig. S4E). Initiation of the UPR^{mt} by thiamphenicol also induced expression of prohibitins and cell cycle genes in C2C12 cells (fig. S4F). These results indicate that NR activates the UPR^{mt} and the prohibitin signaling pathway, as it inhibits MuSC senescence.

NR reprograms senescence prone MuSCs in *Mdx* mice

With continuous muscle regeneration, MuSCs in *Mdx* mice are abnormally active at a young age, leading to MuSC depletion and dysfunction later in life. As a result, primary MuSCs isolated from 14-week-old *Mdx* mice were more intensively and frequently stained with β-galactosidase and had a larger cell size than those of control mice (Fig. 5A and fig. S5, A and B). Similar to the effect in aged animals, NR treatment of *Mdx* mice increased MuSC numbers by ~1.8 fold in vivo (Fig. 5, B to D, and fig. S5, C and D), as also confirmed by PAX7 immunostaining (fig. S5E). Along with the increase in MuSCs, there was an increase in regenerated muscle fibers following NR treatment (Fig. 5E and fig. S5F). We extended this analysis by examining the self-renewal capacity of *Mdx* mouse MuSCs. The cellular redox ratio decreases as MuSCs differentiate (*39*), which can be detected by an increase in 450nm autofluorescence (*40*). In line with NR increasing the number of MuSCs in *Mdx* mice, we found reduced autofluorescence from MuSCs isolated from these animals (Fig. 5, F to H). We performed β-galactosidase staining on primary MuSCs that had been isolated from *Mdx* mice treated or without NR treatment in vivo, and were then further cultured with or without NR in vitro. MuSCs isolated from NR-treated mice were less prone to senescence (Fig. 5I and fig. S5G). When MuSCs isolated from control *Mdx* mice were treated with NR in vitro there was also a reduction in senescence (Fig. 5I and fig. S5G). The inhibition of MuSCs senescence in NR-treated *Mdx* mice was confirmed by the attenuation of. γH2AX and cleaved caspase-3 immunostaining (Fig. 5J). To evaluate MuSC function, CTX-induced muscle regeneration was examined in NR-treated *Mdx* mice. Consistent with the prevention of MuSC senescence, muscle regeneration was improved with NR in both aged (Fig. 5K and fig. S5H) and young *Mdx* mice (fig. S5I). We also examined the effect of NR on the FAP population and muscle regeneration in *Mdx* mice. NR treatment increased MuSCs and reduced FAP numbers in basal conditions and 7 days after CTX-induced damage (fig. S5, J to L). Abnormal activation of FAPs in *Mdx* mice contributes to fibrosis (*31*). *Mdx* mice treated with CTX and then exposed to NR showed lower levels of macrophage infiltration 7 days after damage (fig. S5, M and N). Our results hence indicate a beneficial effect of NR on MuSC function and regeneration in *Mdx* mice.

NR attenuates senescence of neural stem cells and melanocyte stem cells and increases mouse lifespan

Aging is accompanied by a decline in the number and function of neural stem cells (NSCs) (*23*) and melanocyte stem cells (McSCs) (*41*). Therefore, to examine the generalized importance of NAD$^+$ homeostasis in somatic SCs, we assessed the effect of NR in NSCs from aged mice. NR increased proliferation as shown by 5-ethynyl-2-deoxyuridine (EdU) and antigen K_i-67 (Ki67) staining, and induced neurogenesis indicated by doublecortin (DCX) staining, in both the subventricular zone (SVZ) (Fig. 6, A to D) and the dentate gyrus (DG) of the hippocampus (fig. S6, A to D) in aged mice. Nicotinamide mononucleotide (NMN), another NAD$^+$ precursor, also has beneficial effects in aged neural stem cells (*23*). Similarly, NR rescued the decline of McSCs in hair follicles of aged mice, as reflected by increases in mast/stem cell growth factor receptor Kit (c-KIT) and short transient receptor potential channel 2 (TRP2), known McSCs markers, in NR-treated aged mice (Fig. 6, E and F). NR treatment of C57BL/6J mice slightly increased lifespan (chow diet, mean 829 ± 12.0; NR, mean 868 ± 12.4 days, p = 0.034) (Fig. 6G). The beneficial effect of NR on survival was further confirmed by Cox proportional hazards analysis (Fig. 6H). Although the lifespan benefit is small, it was obtained with the NR treatment commencing late in life at 24 months. This argues that aging, in part, may stem from the dysregulation of general SC NAD$^+$ homeostasis.

Conclusions

Oxidative stress, potentially introduced by mitochondrial respiration, is thought to be circumvented in stem cells by their reliance on glycolysis as a primary energy resource (*42*). However, our study demonstrates that mitochondrial oxidative respiration is important for the functional maintenance of multiple types of adult SCs during aging. In fact, the reduction in cellular NAD$^+$ pools blunts the adaptive UPR^{mt} pathway (*18*), ultimately leading to a loss of mitochondrial homeostasis with a concurrent reduction in the number and the self-renewal capacity of MuSCs. Accordingly, by boosting MuSC concentration of NAD$^+$, proteotoxic stress resistance may be restored due to the activation of the UPR^{mt} pathway, stimulating the prohibitin family of mitochondrial stress sensors and effectors. This will in turn improve mitochondrial homeostasis, protecting MuSCs from senescence and safeguarding muscle function in aged mice (fig. S6E). Most importantly, using a MuSC-specific loss-of-function model for *Sirt1*, an essential regulator governing mitochondrial homeostasis (*43*), the importance and essential nature of the relationship between the NAD$^+$-SIRT1 pathway, mitochondrial activity and MuSCs function was

unequivocally established in vivo. Maintaining healthy mitochondria, by replenishing NAD^+ stores, seems furthermore to have beneficial effects beyond MuSCs, and also protect NSC and McSC populations from aging

In combination, our results demonstrate that the depression of prohibitin signaling, leading to mitochondrial dysfunction, can be reversed in aging using a nutritional intervention to boost NAD^+ concentrations in SCs, and suggest that NAD^+ repletion may be revealed as an attractive strategy for improving mammalian lifespan.

REFERENCES AND NOTES

1. A. J. Wagers, I. L. Weissman, Plasticity of adult stem cells. *Cell* **116**, 639–648 (2004). Medline doi:10.1016/S0092-8674(04)00208-9
2. T. Kuilman, C. Michaloglou, W. J. Mooi, D. S. Peeper, The essence of senescence. *Genes Dev.* **24**, 2463–2479 (2010). Medline doi:10.1101/gad.1971610
3. C. López-Otín, M. A. Blasco, L. Partridge, M. Serrano, G. Kroemer, The hallmarks of aging. *Cell* **153**, 1194–1217 (2013). Medline doi:10.1016/j.cell.2013.05.039
4. H. Yin, F. Price, M. A. Rudnicki, Satellite cells and the muscle stem cell niche. *Physiol. Rev.* **93**, 23–67 (2013). Medline doi:10.1152/physrev.00043.2011
5. M. Tabebordbar, E. T. Wang, A. J. Wagers, Skeletal muscle degenerative diseases and strategies for therapeutic muscle repair. *Annu. Rev. Pathol.* **8**, 441–475 (2013). Medline doi:10.1146/annurev-pathol-011811-132450
6. Y. C. Jang, M. Sinha, M. Cerletti, C. Dall'Osso, A. J. Wagers, Skeletal muscle stem cells: Effects of aging and metabolism on muscle regenerative function. *Cold Spring Harb. Symp. Quant. Biol.* **76**, 101–111 (2011). Medline doi:10.1101/sqb.2011.76.010652
7. C. S. Fry, J. D. Lee, J. Mula, T. J. Kirby, J. R. Jackson, F. Liu, L. Yang, C. L. Mendias, E. E. Dupont-Versteegden, J. J. McCarthy, C. A. Peterson, Inducible depletion of satellite cells in adult, sedentary mice impairs muscle regenerative capacity without affecting sarcopenia. *Nat. Med.* **21**, 76–80 (2015). Medline doi:10.1038/nm.3710
8. F. D. Price, J. von Maltzahn, C. F. Bentzinger, N. A. Dumont, H. Yin, N. C. Chang, D. H. Wilson, J. Frenette, M. A. Rudnicki, Inhibition of JAK-STAT signaling stimulates adult satellite cell function. *Nat. Med.* **20**, 1174–1181 (2014). Medline doi:10.1038/nm.3655
9. I. M. Conboy, M. J. Conboy, A. J. Wagers, E. R. Girma, I. L. Weissman, T. A. Rando, Rejuvenation of aged progenitor cells by exposure to a young systemic environment. *Nature* **433**, 760–764 (2005). Medline doi:10.1038/nature03260
10. J. V. Chakkalakal, K. M. Jones, M. A. Basson, A. S. Brack, The aged niche disrupts muscle stem cell quiescence. *Nature* **490**, 355–360 (2012). Medline doi:10.1038/nature11438
11. P. Sousa-Victor, S. Gutarra, L. García-Prat, J. Rodriguez-Ubreva, L. Ortet, V. Ruiz-Bonilla, M. Jardí, E. Ballestar, S. González, A. L. Serrano, E. Perdiguero, P. Muñoz-Cánoves, Geriatric muscle stem cells switch reversible quiescence into senescence. *Nature* **506**, 316–321 (2014). Medline doi:10.1038/nature13013
12. J. D. Bernet, J. D. Doles, J. K. Hall, K. Kelly Tanaka, T. A. Carter, B. B. Olwin, p38 MAPK signaling underlies a cell-autonomous loss of stem cell self-renewal in skeletal muscle of aged mice. *Nat. Med.* **20**, 265–271 (2014). Medline doi:10.1038/nm.3465
13. B. D. Cosgrove, P. M. Gilbert, E. Porpiglia, F. Mourkioti, S. P. Lee, S. Y. Corbel, M. E. Llewellyn, S. L. Delp, H. M. Blau, Rejuvenation of the muscle stem cell population restores strength to injured aged muscles. *Nat. Med.* **20**, 255–264 (2014). Medline doi:10.1038/nm.3464
14. L. Liu, T. H. Cheung, G. W. Charville, B. M. Hurgo, T. Leavitt, J. Shih, A. Brunet, T. A. Rando, Chromatin modifications as determinants of muscle stem cell quiescence and chronological aging. *Cell Reports* **4**, 189–204 (2013). Medline doi:10.1016/j.celrep.2013.05.043
15. M. T. Tierney, T. Aydogdu, D. Sala, B. Malecova, S. Gatto, P. L. Puri, L. Latella, A. Sacco, STAT3 signaling controls satellite cell expansion and skeletal muscle repair. *Nat. Med.* **20**, 1182–1186 (2014). Medline doi:10.1038/nm.3656
16. C. Cantó, R. H. Houtkooper, E. Pirinen, D. Y. Youn, M. H. Oosterveer, Y. Cen, P. J. Fernandez-Marcos, H. Yamamoto, P. A. Andreux, P. Cettour-Rose, K. Gademann, C. Rinsch, K. Schoonjans, A. A. Sauve, J. Auwerx, The NAD^+ precursor nicotinamide riboside enhances oxidative metabolism and protects against high-fat diet-induced obesity. *Cell Metab.* **15**, 838–847 (2012). Medline doi:10.1016/j.cmet.2012.04.022
17. E. Pirinen, C. Cantó, Y. S. Jo, L. Morato, H. Zhang, K. J. Menzies, E. G. Williams, L. Mouchiroud, N. Moullan, C. Hagberg, W. Li, S. Timmers, R. Imhof, J. Verbeek, A. Pujol, B. van Loon, C. Viscomi, M. Zeviani, P. Schrauwen, A. A. Sauve, K. Schoonjans, J. Auwerx, Pharmacological inhibition of poly(ADP-ribose) polymerases improves fitness and mitochondrial function in skeletal muscle. *Cell Metab.* **19**, 1034–1041 (2014). Medline doi:10.1016/j.cmet.2014.04.002
18. L. Mouchiroud, R. H. Houtkooper, N. Moullan, E. Katsyuba, D. Ryu, C. Cantó, A. Mottis, Y. S. Jo, M. Viswanathan, K. Schoonjans, L. Guarente, J. Auwerx, The NAD^+/sirtuin pathway modulates longevity through activation of mitochondrial UPR and FOXO signaling. *Cell* **154**, 430–441 (2013). Medline doi:10.1016/j.cell.2013.06.016
19. J. Yoshino, K. F. Mills, M. J. Yoon, S. Imai, Nicotinamide mononucleotide, a key NAD^+ intermediate, treats the pathophysiology of diet- and age-induced diabetes in mice. *Cell Metab.* **14**, 528–536 (2011). Medline doi:10.1016/j.cmet.2011.08.014
20. A. P. Gomes, N. L. Price, A. J. Ling, J. J. Moslehi, M. K. Montgomery, L. Rajman, J. P. White, J. S. Teodoro, C. D. Wrann, B. P. Hubbard, E. M. Mercken, C. M. Palmeira, R. de Cabo, A. P. Rolo, N. Turner, E. L. Bell, D. A. Sinclair, Declining NAD^+ induces a pseudohypoxic state disrupting nuclear-mitochondrial communication during aging. *Cell* **155**, 1624–1638 (2013). Medline doi:10.1016/j.cell.2013.11.037
21. K. Ito, T. Suda, Metabolic requirements for the maintenance of self-renewing stem cells. *Nat. Rev. Mol. Cell Biol.* **15**, 243–256 (2014). Medline doi:10.1038/nrm3772
22. M. Cerletti, Y. C. Jang, L. W. Finley, M. C. Haigis, A. J. Wagers, Short-term calorie restriction enhances skeletal muscle stem cell function. *Cell Stem Cell* **10**, 515–519 (2012). Medline doi:10.1016/j.stem.2012.04.002
23. L. R. Stein, S. Imai, Specific ablation of Nampt in adult neural stem cells recapitulates their functional defects during aging. *EMBO J.* **33**, 1321–1340 (2014). Medline
24. P. Katajisto, J. Döhla, C. L. Chaffer, N. Pentinmikko, N. Marjanovic, S. Iqbal, R. Zoncu, W. Chen, R. A. Weinberg, D. M. Sabatini, Asymmetric apportioning of aged mitochondria between daughter cells is required for stemness. *Science* **348**, 340–343 (2015). Medline doi:10.1126/science.1260384
25. J. G. Ryall, S. Dell'Orso, A. Derfoul, A. Juan, H. Zare, X. Feng, D. Clermont, M. Koulnis, G. Gutierrez-Cruz, M. Fulco, V. Sartorelli, The NAD^+-dependent SIRT1 deacetylase translates a metabolic switch into regulatory epigenetics in skeletal muscle stem cells. *Cell Stem Cell* **16**, 171–183 (2015). Medline doi:10.1016/j.stem.2014.12.004
26. T. R. Mercer, S. Neph, M. E. Dinger, J. Crawford, M. A. Smith, A. M. Shearwood, E. Haugen, C. P. Bracken, O. Rackham, J. A. Stamatoyannopoulos, A. Filipovska, J. S. Mattick, The human mitochondrial transcriptome. *Cell* **146**, 645–658 (2011). Medline doi:10.1016/j.cell.2011.06.051
27. A. Sickmann, J. Reinders, Y. Wagner, C. Joppich, R. Zahedi, H. E. Meyer, B. Schönfisch, I. Perschil, A. Chacinska, B. Guiard, P. Rehling, N. Pfanner, C. Meisinger, The proteome of *Saccharomyces cerevisiae* mitochondria. *Proc. Natl. Acad. Sci. U.S.A.* **100**, 13207–13212 (2003). Medline
28. D. J. Pagliarini, S. E. Calvo, B. Chang, S. A. Sheth, S. B. Vafai, S. E. Ong, G. A. Walford, C. Sugiana, A. Boneh, W. K. Chen, D. E. Hill, M. Vidal, J. G. Evans, D. R. Thorburn, S. A. Carr, V. K. Mootha, A mitochondrial protein compendium elucidates complex I disease biology. *Cell* **134**, 112–123 (2008). Medline
29. R. H. Houtkooper, C. Cantó, R. J. Wanders, J. Auwerx, The secret life of NAD^+: An old metabolite controlling new metabolic signaling pathways. *Endocr. Rev.* **31**, 194–223 (2010). Medline doi:10.1210/er.2009-0026
30. S. Sartore, L. Gorza, S. Schiaffino, Fetal myosin heavy chains in regenerating muscle. *Nature* **298**, 294–296 (1982). Medline doi:10.1038/298294a0
31. D. R. Lemos, F. Babaeijandaghi, M. Low, C. K. Chang, S. T. Lee, D. Fiore, R. H. Zhang, A. Natarajan, S. A. Nedospasov, F. M. Rossi, Nilotinib reduces muscle fibrosis in chronic muscle injury by promoting TNF-mediated apoptosis of fibro/adipogenic progenitors. *Nat. Med.* **21**, 786–794 (2015). Medline doi:10.1038/nm.3869

32. E. Hara, R. Smith, D. Parry, H. Tahara, S. Stone, G. Peters, Regulation of p16CDKN2 expression and its implications for cell immortalization and senescence. *Mol. Cell. Biol.* **16**, 859–867 (1996). Medline doi:10.1128/MCB.16.3.859
33. L. C. Gillet, P. Navarro, S. Tate, H. Röst, N. Selevsek, L. Reiter, R. Bonner, R. Aebersold, Targeted data extraction of the MS/MS spectra generated by data-independent acquisition: A new concept for consistent and accurate proteome analysis. *Mol. Cell. Proteomics* **11**, 0111.016717 (2012). Medline doi:10.1074/mcp.O111.016717
34. P. Rimmelé, R. Liang, C. L. Bigarella, F. Kocabas, J. Xie, M. N. Serasinghe, J. Chipuk, H. Sadek, C. C. Zhang, S. Ghaffari, Mitochondrial metabolism in hematopoietic stem cells requires functional FOXO3. *EMBO Rep.* **16**, 1164–1176 (2015). Medline doi:10.15252/embr.201439704
35. P. J. Coates, R. Nenutil, A. McGregor, S. M. Picksley, D. H. Crouch, P. A. Hall, E. G. Wright, Mammalian prohibitin proteins respond to mitochondrial stress and decrease during cellular senescence. *Exp. Cell Res.* **265**, 262–273 (2001). Medline doi:10.1006/excr.2001.5166
36. P. J. Coates, D. J. Jamieson, K. Smart, A. R. Prescott, P. A. Hall, The prohibitin family of mitochondrial proteins regulate replicative lifespan. *Curr. Biol.* **7**, 607–610 (1997). Medline doi:10.1016/S0960-9822(06)00261-2
37. M. Artal-Sanz, N. Tavernarakis, Prohibitin couples diapause signalling to mitochondrial metabolism during ageing in *C. elegans*. *Nature* **461**, 793–797 (2009). Medline doi:10.1038/nature08466
38. C. Osman, C. Merkwirth, T. Langer, Prohibitins and the functional compartmentalization of mitochondrial membranes. *J. Cell Sci.* **122**, 3823–3830 (2009). Medline doi:10.1242/jcs.037655
39. M. Fulco, R. L. Schiltz, S. Iezzi, M. T. King, P. Zhao, Y. Kashiwaya, E. Hoffman, R. L. Veech, V. Sartorelli, Sir2 regulates skeletal muscle differentiation as a potential sensor of the redox state. *Mol. Cell* **12**, 51–62 (2003). Medline doi:10.1016/S1097-2765(03)00226-0
40. K. P. Quinn, G. V. Sridharan, R. S. Hayden, D. L. Kaplan, K. Lee, I. Georgakoudi, Quantitative metabolic imaging using endogenous fluorescence to detect stem cell differentiation. *Sci. Rep.* **3**, 3432 (2013). Medline doi:10.1038/srep03432
41. E. K. Nishimura, S. R. Granter, D. E. Fisher, Mechanisms of hair graying: Incomplete melanocyte stem cell maintenance in the niche. *Science* **307**, 720–724 (2005). Medline doi:10.1126/science.1099593
42. C. D. Folmes, P. P. Dzeja, T. J. Nelson, A. Terzic, Metabolic plasticity in stem cell homeostasis and differentiation. *Cell Stem Cell* **11**, 596–606 (2012). Medline doi:10.1016/j.stem.2012.10.002
43. C. Cantó, K. J. Menzies, J. Auwerx, NAD$^+$ metabolism and the control of energy homeostasis: A balancing act between mitochondria and the nucleus. *Cell Metab.* **22**, 31–53 (2015). Medline doi:10.1016/j.cmet.2015.05.023
44. M. F. Champy, M. Selloum, V. Zeitler, C. Caradec, B. Jung, S. Rousseau, L. Pouilly, T. Sorg, J. Auwerx, Genetic background determines metabolic phenotypes in the mouse. *Mamm. Genome* **19**, 318–331 (2008). Medline doi:10.1007/s00335-008-9107-z
45. P. Rebora, A. Salim, M. Reilly, bshazard: A flexible tool for nonparametric smoothing of the hazard function. *R J.* **6**, 114 (2014).
46. T. M. Therneau, P. M. Grambsch, *Modeling Survival Data: Extending the Cox Model* (Springer, New York, 2000).
47. E. Kimura, S. Li, P. Gregorevic, B. M. Fall, J. S. Chamberlain, Dystrophin delivery to muscles of *mdx* mice using lentiviral vectors leads to myogenic progenitor targeting and stable gene expression. *Mol. Ther.* **18**, 206–213 (2010). Medline doi:10.1038/mt.2009.253
48. Y. Wu, E. G. Williams, S. Dubuis, A. Mottis, V. Jovaisaite, S. M. Houten, C. A. Argmann, P. Faridi, W. Wolski, Z. Kutalik, N. Zamboni, J. Auwerx, R. Aebersold, Multilayered genetic and omics dissection of mitochondrial activity in a mouse reference population. *Cell* **158**, 1415–1430 (2014). Medline doi:10.1016/j.cell.2014.07.039
49. H. Lam, E. W. Deutsch, J. S. Eddes, J. K. Eng, N. King, S. E. Stein, R. Aebersold, Development and validation of a spectral library searching method for peptide identification from MS/MS. *Proteomics* **7**, 655–667 (2007). Medline doi:10.1002/pmic.200600625
50. B. C. Collins, L. C. Gillet, G. Rosenberger, H. L. Röst, A. Vichalkovski, M. Gstaiger, R. Aebersold, Quantifying protein interaction dynamics by SWATH mass spectrometry: Application to the 14-3-3 system. *Nat. Methods* **10**, 1246–1253 (2013). Medline doi:10.1038/nmeth.2703
51. H. L. Röst, G. Rosenberger, P. Navarro, L. Gillet, S. M. Miladinović, O. T. Schubert, W. Wolski, B. C. Collins, J. Malmström, L. Malmström, R. Aebersold, OpenSWATH enables automated, targeted analysis of data-independent acquisition MS data. *Nat. Biotechnol.* **32**, 219–223 (2014). Medline doi:10.1038/nbt.2841
52. L. Reiter, O. Rinner, P. Picotti, R. Hüttenhain, M. Beck, M. Y. Brusniak, M. O. Hengartner, R. Aebersold, mProphet: Automated data processing and statistical validation for large-scale SRM experiments. *Nat. Methods* **8**, 430–435 (2011). Medline doi:10.1038/nmeth.1584
53. J. A. Vizcaíno, A. Csordas, N. Del-Toro, J. A. Dianes, J. Griss, I. Lavidas, G. Mayer, Y. Perez-Riverol, F. Reisinger, T. Ternent, Q. W. Xu, R. Wang, H. Hermjakob, 2016 update of the PRIDE database and its related tools. *Nucleic Acids Res.* **44**, D447–D456 (2016). Medline doi:10.1093/nar/gkv1145
54. M. Watanabe, S. M. Houten, C. Mataki, M. A. Christoffolete, B. W. Kim, H. Sato, N. Messaddeq, J. W. Harney, O. Ezaki, T. Kodama, K. Schoonjans, A. C. Bianco, J. Auwerx, Bile acids induce energy expenditure by promoting intracellular thyroid hormone activation. *Nature* **439**, 484–489 (2006). Medline doi:10.1038/nature04330

ACKNOWLEDGMENTS

HZ, DR, KJM, JA, and the EPFL have filed a provisional patent application on the use of NAD boosting to enhance stem cell function. We thank T. Langer for kindly sharing the *Phb* plasmids; S. Wang and M. Knobloch for technical help in melanocyte and neural stem cell experiments; H. Li, L. Mouchiroud, P. Moral Quiros, and all members of the Auwerx and Schoonjans groups, for helpful discussions. HZ is the recipient of a doctoral scholarship from the China Scholarship Council (CSC) and a fellowship from CARIGEST SA. DD was supported by fellowship from Associazione Italiana per la Ricerca sul Cancro (AIRC). KJM is supported by the University of Ottawa and the Heart and Stroke Foundation of Canada. JA is the Nestlé Chair in Energy Metabolism and his research is supported by EPFL, NIH (R01AG043930), Krebsforschung Schweiz/SwissCancerLeague (KFS-3082-02-2013), Systems X (SySX.ch 2013/153) and SNSF (31003A-140780). The technical assistance from the EPFL histology and flow cytometry core facilities was greatly appreciated.

SUPPLEMENTARY MATERIALS

www.sciencemag.org/cgi/content/full/science.aaf2693/DC1
Materials and Methods
Figs. S1 to S6
Tables S1 to S6
References (*44*–*54*)

16 January 2016; accepted 13 April 2016
Published online 28 April 2016
10.1126/science.aaf2693

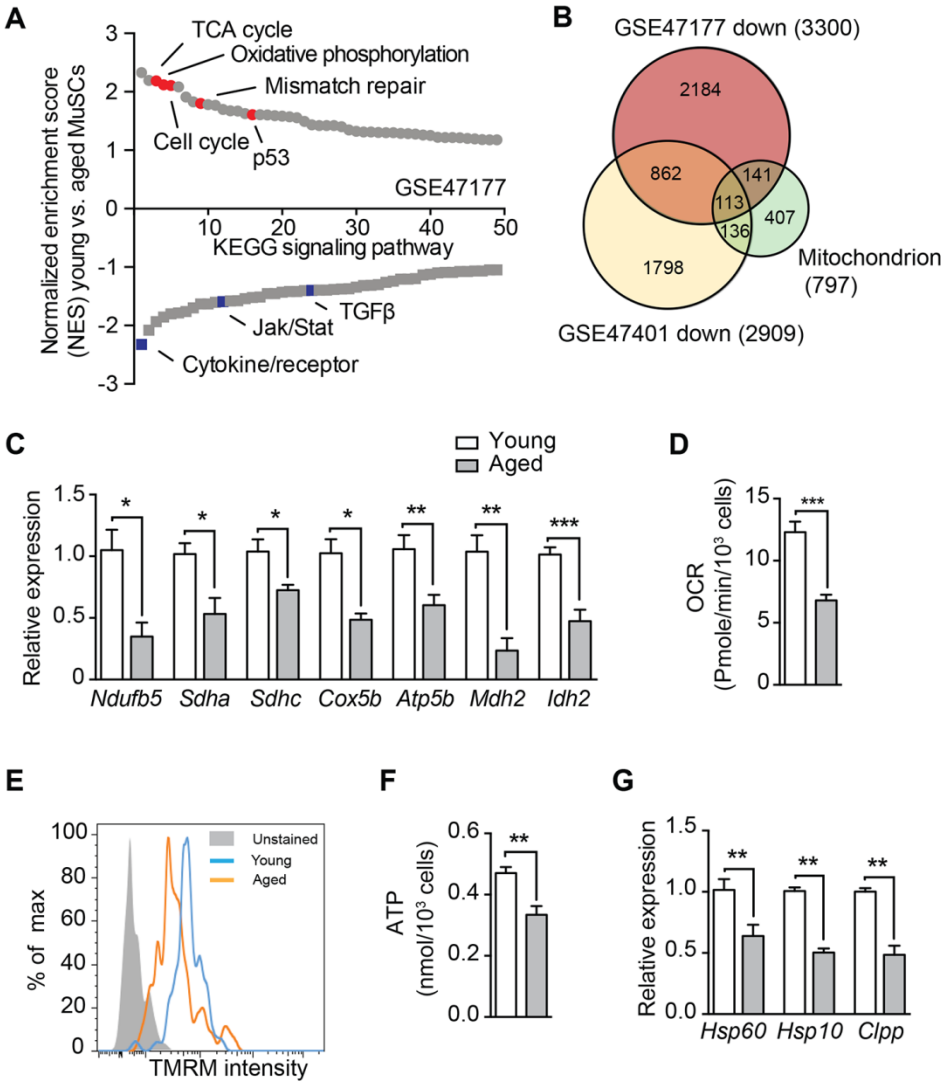

Fig. 1. Mitochondrial dysfunction in muscle stem cells (MuSCs) during aging. (**A**) Gene-set enrichment analysis (GSEA) demonstrates up- and downregulated signaling pathways in MuSCs from two-year-old mice, compared to four-month-old mice. Analysis of microarray data from the publicly available GEO data set (accession number GSE47177) using Kyoto encyclopedia of genes and genomes (KEGG) enrichment. Signaling pathways were ranked on the basis of normalized enrichment scores (NESs); positive and negative NESs indicate down- or upregulation in aged MuSCs, respectively. Specific pathways related to MuSC function are highlighted in red and blue. (**B**) Area-proportional Venn diagram representing 113 common genes between the significantly downregulated genes ($p < 0.05$) in MuSC transcriptomes originating from aged mice [GSE47177 and GSE47401 (*12*)], and genes from the human mitochondrial transcriptome (*26*). (**C** to **G**) Young (1 month old) and aged (22-24 months old) C57BL/6J mice received a dietary supplement with NR for 6 weeks. (C) qRT-PCR validation of transcriptional changes in mitochondrial genes of freshly sorted MuSCs. (D) Oxygen consumption rate (OCR) in freshly isolated MuSCs, following 16h of recovery at 37°C. (E and F) Mitochondrial membrane potential, measured by tetramethylrhodamine, methyl ester (TMRM) assay (H) and cellular ATP levels (I) in freshly isolated MuSCs. (G) Relative gene expression for UPR^{mt} genes and cell senescence markers in freshly sorted MuSCs. Data are normalized to *36b4* mRNA transcript levels. All statistical significance was calculated by Student's *t* test. All data are shown as mean ± SEM. *$p < 0.05$, **$p < 0.01$, ***$p < 0.001$. [(C), (D), (F), and (G)] $n = 6$; (E) $n = 3$ mice per group.

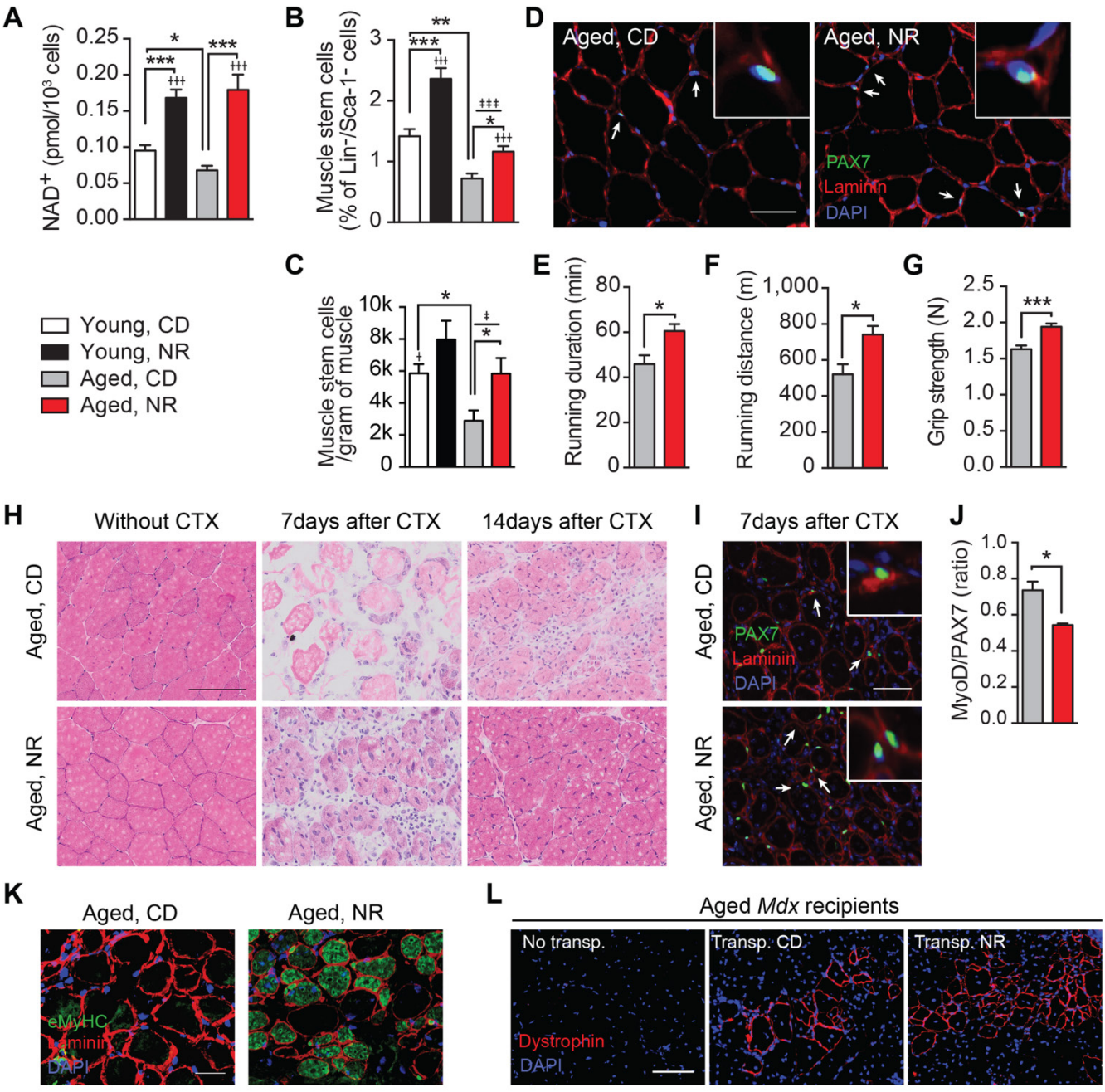

Fig. 2. Improved muscle stem cell numbers and muscle function in NR-treated aged mice. Young (3 months old) and aged (22-24 months old) C57BL/6J mice received chow diet (CD) or CD supplement with NR for 6 weeks. All results are compared to age-matched mice given a control diet. (**A**) NAD^+ concentrations in freshly isolated MuSCs. (**B** and **C**) Percentage of FACS quantified $CD34^+$/integrin $\alpha7^+$/Lin^-/$Sca\text{-}1^-$ MuSCs relative to the total Lin^-/$Sca\text{-}1^-$ cell population (B) or to muscle weight (C). (**D**) Representative images of PAX7 and laminin immunostained tibialis anterior (TA) muscle. Arrows point to PAX7-positive SCs. 20 × 20 μm insets show a single MuSC. Scale bar = 50 μm. (**E** to **G**) Comparison of maximal running duration (E), running distance (F) and grip strength (G) in NR-treated aged mice. (**H**) H&E stained TA tissue-sections from NR-treated aged mice 7 and 14 days after cardiotoxin (CTX)-induced muscle damage. Scale bar = 100 μm. (**I**) Images of PAX7 and laminin immunostained TA muscle cross-sections taken from NR-treated aged mice 7 days after CTX-induced muscle damage. Arrows point to PAX7-positive MuSCs. 20 × 20 μm insets show a single MuSC. Scale bar = 50 μm. (**J**) Quantification of the signal intensity ratio between MYOD1 and PAX7 in PAX7-positive MuSCs, performed on sections isolated 7 days after muscle damage in aged mice. Images not shown. (**K**) Newly regenerated muscle fibers, stained by embryonic myosin heavy chain (eMyHC) 7 days after muscle damage in aged mice. Scale bar = 50 μm. (**L**) Dystrophin immunostaining of TA muscle sections in aged (16 months old) *Mdx* mice 4-weeks after receiving transplantations of MuSCs isolated from control or NR-treated aged C56BL/6J donors. Scale bar = 100μm. All statistical significance was calculated by Student's *t* test or two-way ANOVA. All data are shown as mean ± SEM. $*p < 0.05$, $**p < 0.01$, $***p < 0.001$. Main effects for treatment or age are denoted as † or ‡, respectively, with interactions denoted as ε. (A) $n = 6$ mice; [(B) to (D) and (H) to (K)] $n = 3$-6 mice per group; [(E) to (G)] $n = 10$ control diet; $n = 7$ NR-treated mice; (L) $n = 12$ donor mice, $n = 3$ recipient mice for each treatment. Corresponding young control data for (E) to (I), are found in fig. S2, J to O, respectively.

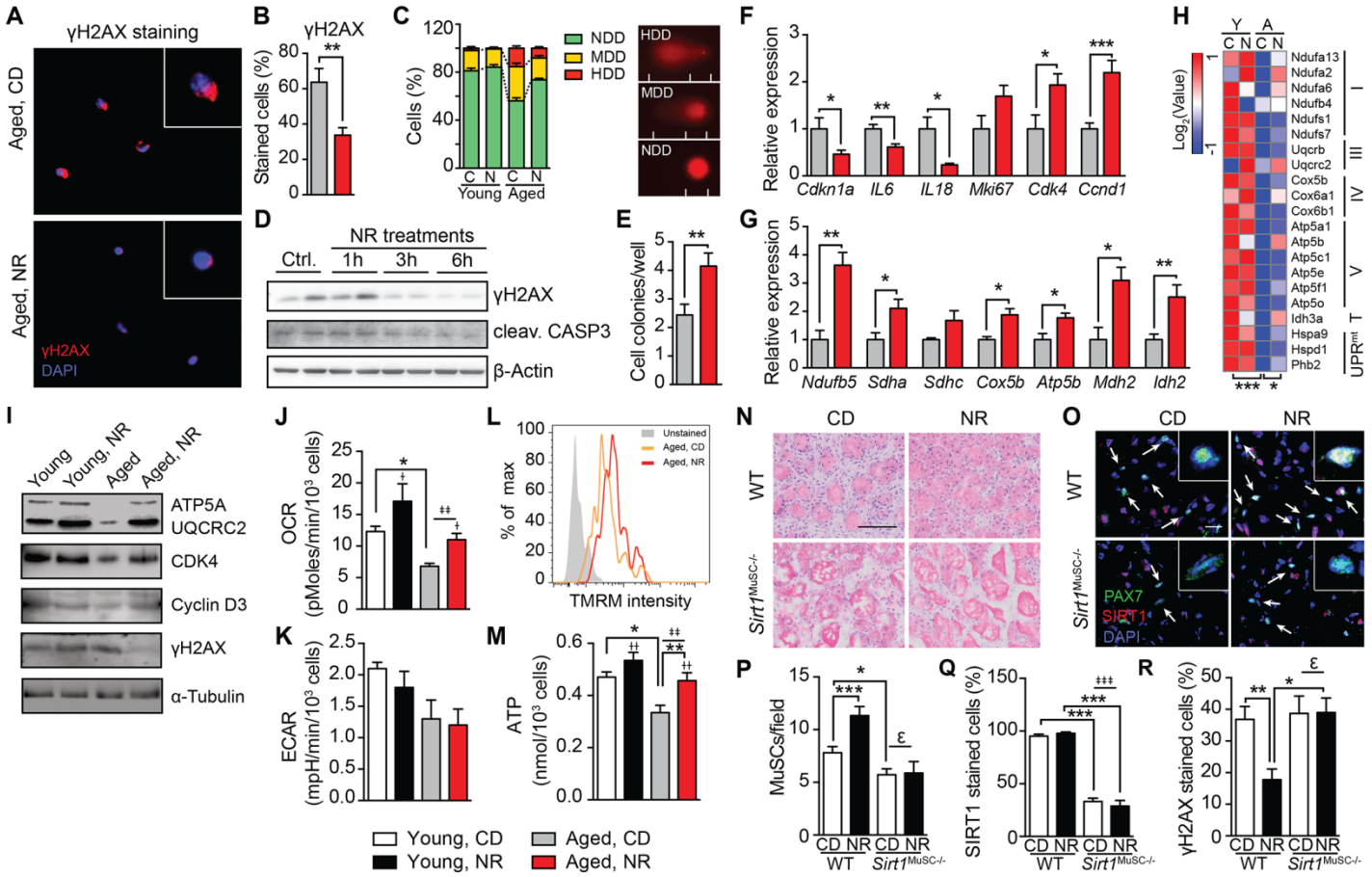

Fig. 3. NR treatment prevents MuSC senescence and improves mitochondrial function. Aged (22-24 months old) C57BL/6J mice or 8 months old SIRT1$^{MuSC-/-}$ mice received a dietary supplement with NR for 6 weeks. All isolated MuSCs were freshly FACS sorted for assay. Most comparative data from young mice (1 month old) are presented in fig. S3. (**A** and **B**) Immunostaining (A) and quantification (B) of γH2AX staining in freshly sorted MuSCs from aged mice. 20 × 20 μm insets show single MuSCs. (**C**) Single-cell gel electrophoresis (comet) assay of MuSCs from aged mice. C, chow diet; N, NR treated. NDD, non-damaged DNA; MDD, moderately-damaged DNA; HDD, heavily-damaged DNA. (**D**) Proteins levels in C2C12 myoblasts with NR treatment for 1, 3, or 6 hours. (**E**) Colony formation ability assay in isolated MuSCs. (**F** and **G**) Quantification of transcript expression for cell cycle and inflammatory secretome genes (F) or OXPHOS and TCA cycle genes (G) in MuSCs. (**H**) Abundance of proteins from MuSCs of young (Y) and aged (A) mice fed with a chow (C) or NR diet (N). Protein abundance was calculated using peptide intensity detected in the SWATH-MS map. Roman numerals indicate corresponding OXPHOS complexes. T, TCA cycle. (**I**) Protein levels in MuSCs. (**J** and **K**) OCR (J) and ECAR (K), in MuSCs following 16 h of recovery at 37°C. (**L**) Mitochondrial membrane potential, measured by a TMRM assay in MuSCs. (**M**) Cellular ATP concentration in MuSCs. (**N**) H&E stained TA muscle from wild type or SIRT1$^{MuSC-/-}$ mice 7 days after cardiotoxin (CTX)-induced muscle damage. Scale bar = 100 μm. (**O** to **Q**) Representative images (O) and quantification of PAX7-positive MuSCs in random fields of view (160 × 160 μm) (P) and the percentage of SIRT1-positive MuSCs (Q) in immunostained TA 7 days after CTX-induced muscle damage. Arrows point to PAX7-positive MuSCs. 20 × 20 μm insets show a single MuSC. Scale bar = 50 μm. (**R**) Quantification of γH2AX-positive MuSCs in immunostained TA 7 days after CTX-induced muscle damage. All statistical significance was calculated by Student's *t* test or two-way ANOVA. All data are represented as mean ± SEM. $*p < 0.05$, $**p < 0.01$, $***p < 0.001$. Main effects for treatment or age are denoted as † or ‡, respectively, with interactions denoted as ε. [(A) to (C) and (N) to (R)] n = 3-6 mice per group; (E) n = 24 in each group; [(F) and (G) and (J) to (M)] n = 6 mice per group; (H) protein extracted and pooled from 6 mice in each group. Corresponding young control data found in (A), (B), (E), (F), (G), and (L) are found in fig. S3, A, B, D, E, F, and G, respectively.

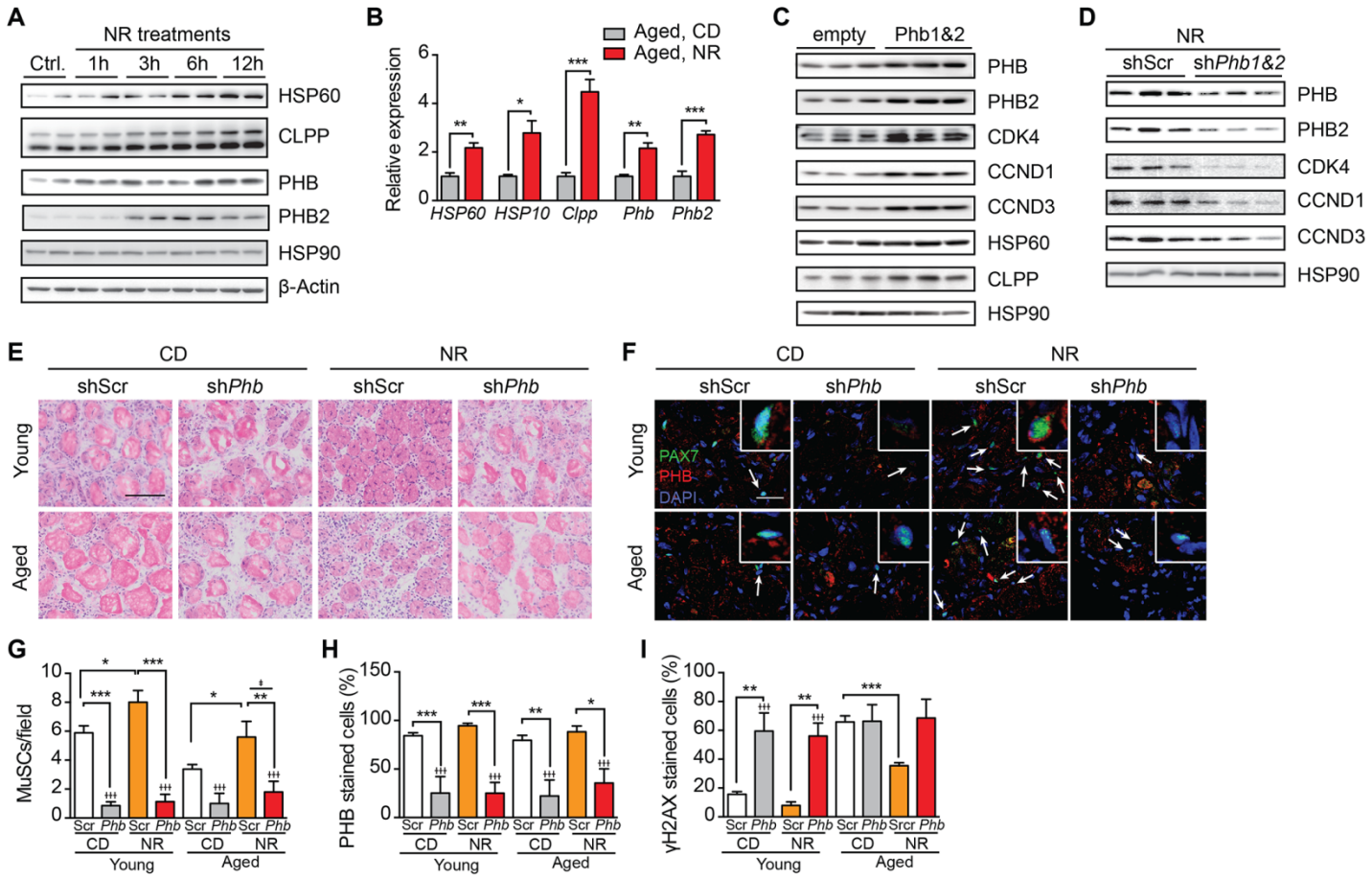

Fig. 4. Effects of NR on prohibitins, UPR^{mt} and MuSC senescence. (**A**) Expression of HSP60, CLPP and prohibitins in C2C12 myoblasts upon NR treatment at the indicated time points. (**B**) Quantification of transcript expression for UPR^{mt} and prohibitin genes in MuSCs from aged (22-24 months old) C57BL/6J mice following 6 weeks of chow or NR diets. (**C**) Expression of prohibitins and cell cycle proteins in C2C12 myoblasts with the combined overexpression of *Phb* and *Phb2*. (**D**) Expression of prohibitins and cell cycle genes with a 6-hour NR treatment in C2C12 myoblasts after a combined *Phb* and *Phb2* shRNA knockdown. (**E**) H&E staining of TA muscle in NR-treated or intramuscular sh*Phb* lentivirus-injected C57BL/6J mice 7 days of after cardiotoxin (CTX)-induced muscle damage. Scale bar = 100 μm. (**F** to **H**) Representative images (F) and quantification of PAX7-positive MuSCs in randomly chosen field of views (160 × 160 μm) (G) and the percentage of PHB-positive MuSCs (H) in immunostained TA muscle 7 days after CTX-induced muscle damage. Arrows point to PAX7-positive MuSCs. 20 × 20 μm insets show single MuSC. Scale bar = 50 μm. (**I**) Quantification of γH2AX-positive MuSCs in immunostained TA muscle cross-sections taken from control and NR-treated mice 7 days after CTX-induced muscle damage. All statistical significance was calculated by Student's *t* test or two-way ANOVA. All data are represented as mean ± SEM. **p* < 0.05, ***p* < 0.01, ****p* < 0.001. Main effects for treatment or age are denoted as † or ‡, respectively, with interactions denoted as ε. (B) *n* = 6 mice; [(E) to (I)] *n* = 3 mice per group. Corresponding young control data found in (B) are found in fig. S4B.

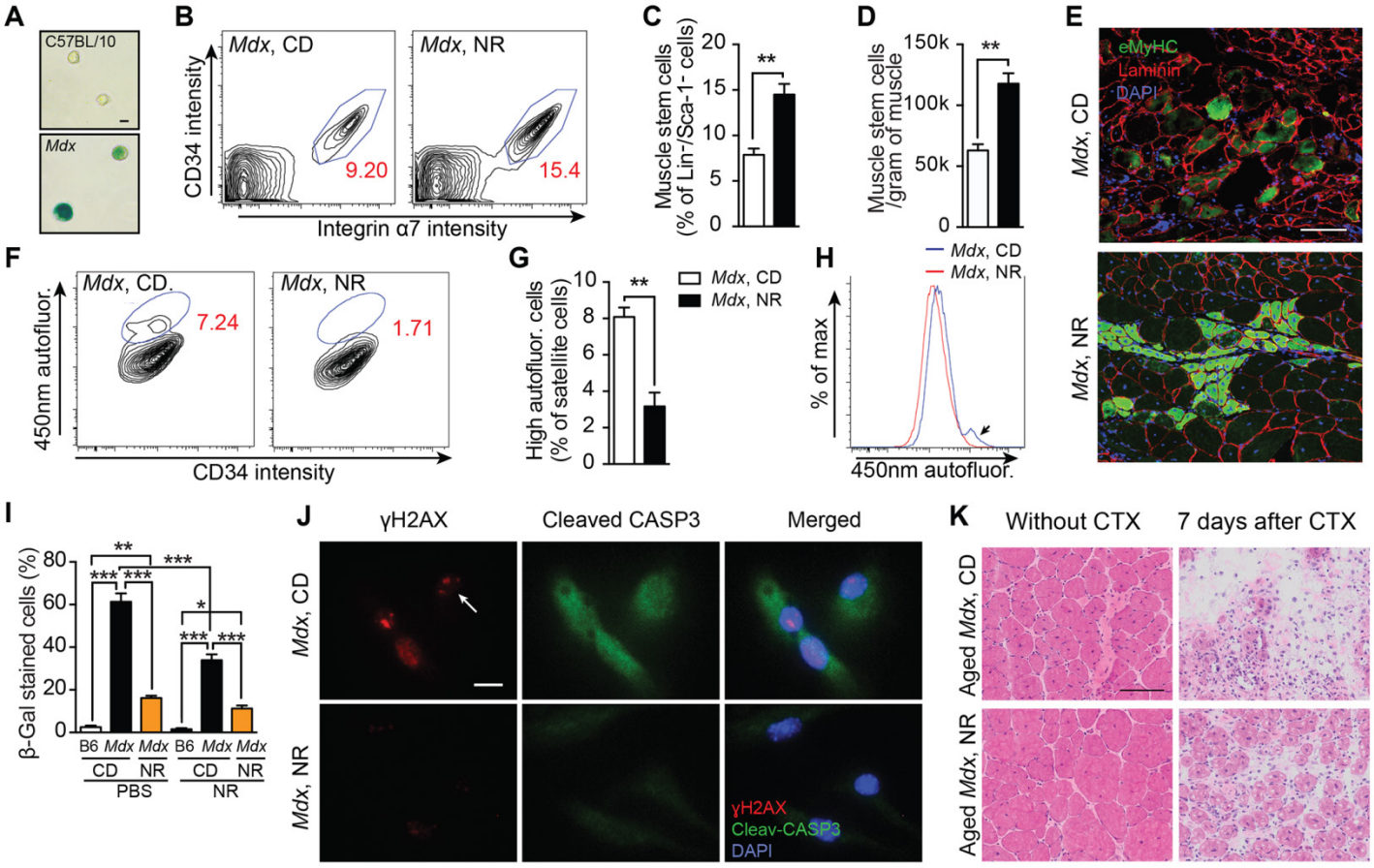

Fig. 5. Increased stem cell number and function in NR-treated *Mdx* mice. *Mdx* mice received a dietary supplement with NR for 10 weeks. All results were compared to *Mdx* mice given a control diet. (**A**) β-galactosidase staining of MuSCs isolated from C57BL/10SnJ or *Mdx* mice and cultured in vitro for three generations. Scale bar = 10 μm. (**B** to **D**) FACS contour plots of Sca-1$^-$/Lin$^-$ cells isolated from muscle. Percentage of the CD34$^+$/integrin α7$^+$/Lin$^-$/Sca-1$^-$ MuSC populations are noted in red in contour plots (B), and quantified relative to the total Lin$^-$/Sca-1$^-$ cell population (C) or to muscle weight (D). (**E**) Immunostaining of and eMyHC$^+$ fibers in tissue-sections of NR-treated *Mdx* mice 7 days after CTX-induced muscle damage. (**F** to **H**) FACS contour plots (F), quantification (G) and distribution (H) of MuSC autofluorescence as a measure of the relative NAD(P)H concentration upon UV light excitation. Autofluorescence emission was detected using 405/450 nm. Arrow in (H) points to the highly autofluorescent stem cell population. (**I**) Quantification of β-galactosidase staining of FACS-sorted MuSCs from C57BL/6J (B6), untreated (*Mdx*) or NR-treated *Mdx* (*Mdx* with NR) mice challenged with PBS or NR for 6 hours in vitro. (**J**) Immunostaining showing γH2AX and cleaved caspase-3 in MuSCs cultured in vitro for three generations. Arrow points to a γH2AX-positive nucleus. Scale bar = 10 μm. (**K**) H&E staining of tissue-sections from NR-treated aged *Mdx* mice (16 months old) with 7 days of recovery following CTX induced muscle damage. Scale bar = 100 μm. All statistical significance was calculated by Student's *t* test or one-way ANOVA. All data are represented as mean ± SEM. **p* < 0.05, ***p* < 0.01, ****p* < 0.001. [(A) to (H), (J), and (K)] *n* = 3-5 per treated group; (I) *n* = 3 mice and *n* = 6 in vitro treatments. More than 500 cells were quantified in each condition.

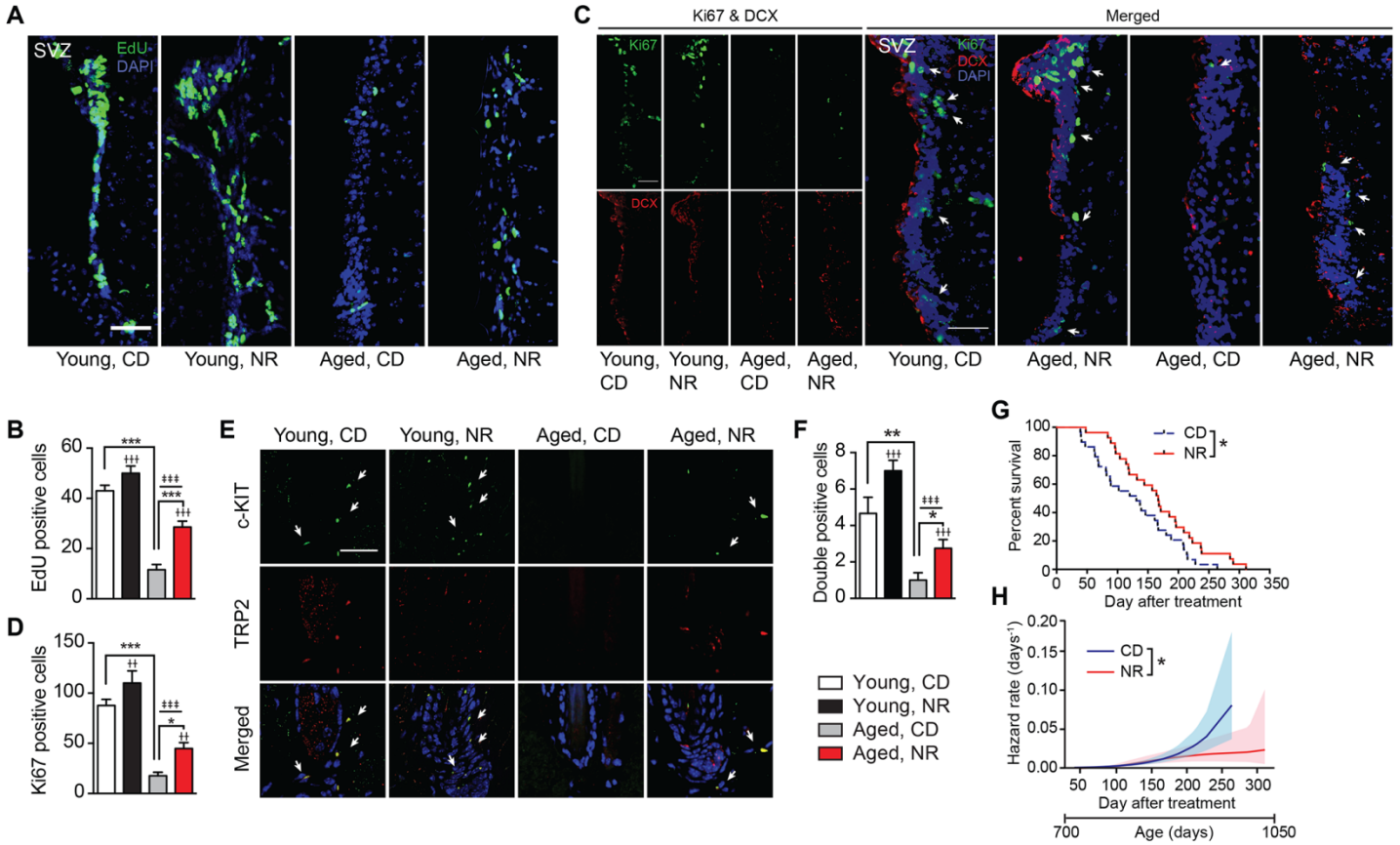

Fig. 6. NR improves neural and melanocyte stem cell (NSC and McSC) function and increases the lifespan of aged C57BL/6J mice. Aged (22-24 months old) C57BL/6J mice received a dietary supplement with NR for 6 weeks. (**A** and **B**) Representative images (A) and quantification (B) of EdU-positive NSCs in the subventricular zone (SVZ) from young and aged mice following NR treatment. Scale bar = 50 μm. (**C** and **D**) Representative images (C) and quantification of Ki67- and doublecortin (DCX)-positive NSCs in the subventricular zone (SVZ) harvested from young and aged mice treated with or without NR (D). Arrows point to Ki67-positive NSCs. Scale bar = 50 μm. (**E** and **F**) Representative images (E) and quantification (F) of c-KIT and TRP2 double positive McSCs in the bulge of hair follicles from dorsal skin harvested from young and aged mice treated with or without NR. Arrows point to double positive McSCs. Scale bar = 50 μm. (**G**) Kaplan-Meier survival curves of control- and NR-treated aged mice, with the NR treatment beginning at 2 years (700 days) of age. (**H**) Hazard rate decreased under NR treatment. Individual lifespans were collected and used to estimate the hazard function of each population using numerical differentiation of the Kaplan–Meier survival estimator (solid lines). The shaded areas represent the 95% confidence bands of the true hazard. The *p* value was calculated with the use of a Cox proportional hazards model. All statistical significance was calculated by Student's *t* test or two-way ANOVA, except in (G) and (H). All data are represented as mean ± SEM. **p* < 0.05, ***p* < 0.01, ****p* < 0.001. Main effects for treatment or age are denoted as † or ‡, respectively, with interactions denoted as ε. [(A) to (F)] *n* = 6; (H) *n* = 30 per treated group.

NAD$^+$ repletion improves mitochondrial and stem cell function and enhances life span in mice

Hongbo Zhang, Dongryeol Ryu, Yibo Wu, Karim Gariani, Xu Wang, Peiling Luan, Davide D'Amico, Eduardo R. Ropelle, Matthias P. Lutolf, Ruedi Aebersold, Kristina Schoonjans, Keir J. Menzies and Johan Auwerx (April 28, 2016)

published online April 28, 2016

Editor's Summary

Science (print ISSN 0036-8075; online ISSN 1095-9203) is published weekly, except the last week in December, by the American Association for the Advancement of Science, 1200 New York Avenue NW, Washington, DC 20005.